Ion momentum distributions for He single and double ionization in strong laser fields

J. Chen and C. H. Nam
Department of Physics and Coherent X-Ray Research Center, Korea Advanced Institute of Science and Technology, Taejon 305-701, Korea

(Received 3 April 2002; published 25 November 2002)

Using a semiclassical rescattering model, the momentum distributions of recoil ions from laser induced single and double ionization are obtained. Not only in the case of double ionization but also in the case of single ionization, the distributions of the momentum parallel to the polarization direction of the laser field show a double-hump structure as a consequence of the rescattering. By comparing with experimental data we find that, as the intensity of the laser decreases, the rescattering ionization mechanism of the second electron as calculated within our model does not dominate the process. In addition, the correlated emission of the electrons in the double ionization is discussed and the effect of the repulsion between the emitted electrons is shown.

DOI: 10.1103/PhysRevA.66.053415 PACS number(s): 32.80.Rm, 32.80.Fb, 34.50.Rk

INTRODUCTION

Among the achievements in the field of interaction between atoms and intense laser pulses, the recognition of the rescattering process [1–3] was one of the most important steps to advance the understanding of the behavior of atoms in laser field. The rescattering process can be understood from a simple quasiclassical notion: once an electron subject to a strong field has undergone a transition into continuum from its initial bound state, its motion is dominated by its interaction with the laser field. In the case of linearly polarized laser field, a majority of these electrons will be driven back into the vicinity of the ion core and undergo elastic or inelastic scattering, or recombine with the core and emit a high-energy photon. This mechanism is the so-called rescattering process. It is commonly believed that rescattering is responsible for many distinct experimental observations, such as the cutoff in high-order harmonic generation, a plateau formed by high-order above-threshold ionization (ATI) peaks [1,2] and the singular angular distributions of the photoelectrons in the plateau regime [3–8].

Since a surprisingly high ion yield in double and multiple ionization of atoms in intense, linearly polarized laser pulses was first observed [9], many-electron dynamics in intense laser fields has been studied intensively both in theoretical and experimental investigations. Especially in recent years, double and multiple ionization of rare-gas atoms in intense laser fields has attracted more and more attention. It is well known that double ionization can occur either by a stepwise process or by so-called nonsequential double-ionization (NSDI) mechanisms. It is commonly accepted that in the stepwise process occurring mainly above the saturation intensity for the single ionization (the intensity at which the neutral target atoms are fully depleted in the interaction volume), the electrons are ionized sequentially, i.e., the probability of the stepwise double ionization is determined by the independent product of the probability of single ionization of the neutral atoms and that of the singly charged ions. In contrast, the mechanism of NSDI, which occurs primarily in the intensity domain near and below the saturation intensity, is still under dispute [2,10–21].

Among the various mechanisms developed, three are rather important. Fittinghoff *et al.* [10] suggested that the second electron could be shaken off by a nonadiabatic change of the potential caused by the emission of the first electron. This mechanism is known to dominate the double ionization of helium after the absorption of single photons with energies beyond 1 keV [22]. The rescattering process has also been proposed to explain NSDI by Corkum [2] and Kuchiev [19]. In this model, the second electron is ionized due to a collision of the first tunneled electron with the parent ion after free propagation during about half an optical cycle in the external laser field. Becker and Faisal [15,23] proposed a ''correlated energy sharing'' model based on the intense-field many-body *S*-matrix theory, derived by rearranging the usual *S*-matrix series. This model includes short-time electron correlation and the rescattering mechanism.

Recently, measurements of the distributions of the recoil momentum of doubly charged He [24], Ne [25], and Ar [26–29] in the NSDI region have been reported and have led to intensive theoretical and experimental investigations on the topic during the last two years [30–46]. In the NSDI region, all the distributions show a remarkably broad double-hump distribution for the recoil momentum parallel to the laser field polarization direction and a narrow single-hump distribution in the perpendicular direction. These characteristic features are believed to serve as a test of various models and rule out the mechanisms based on an instantaneous release of two (or more) electrons at a phase where the field maximizes, such as ''shaken-off'' and ''collective tunneling'' [31]. It is already known that the positions of these maxima are consistent with kinematical constraints set by the ''rescattering model'' [25,30,33,34,36].

In this paper, we calculate the recoil momentum of singly and doubly ionized ions of He using a semiclassical rescattering model developed recently [37]. This model has been applied to quantitatively reproduce the excessive double ionization of He observed in experiments and has gained success in the explanation of the momentum distribution of recoiled He^{2+} ions [36,37]. This model has also been used to study the photoelectron spectra, angular distribution, and correlated electron emission in NSDI [45,46].

THEORY

We begin by briefly presenting the semiclassical rescattering model adopted in the previous calculations [36,37]. The ionization of the first electron from a bound to continuum state is treated by tunneling ionization theory. The subsequent evolution of the ionized electron and the bound electron in the combined Coulomb potential and laser field is described by the classical Newtonian equations. To emulate the evolution of the electron wave packet, a set of trajectories is launched with initial conditions obtained from the wave function of the tunneled electron.

Evolution of the two-electron system after the tunnel ionization of the first electron is determined by the classical equations of motion (in atomic units),

$$\frac{d^2\mathbf{r}_i}{dt^2} = \mathbf{E}(t) - \nabla(V_{ne} + V_{ee}). \tag{1}$$

Here $\mathbf{E}(t) = (0,0,F(t))$ is the electric field and $F(t) = F\cos(\omega t)$. The indices $i = 1$ and 2 refer to the tunnel ionized and the bound electron with ionization potentials I_{p1} and I_{p2}, respectively. The potentials are $V_{ne} = -2/|\mathbf{r}_i|$ and $V_{ee} = 1/|\mathbf{r}_1 - \mathbf{r}_2|$, respectively.

The initial condition of the first, i.e., the tunneled electron, is determined by an equation including an effective potential [36,37]. The initial velocities are set to be $v_z = 0, v_x = v_{per}\cos(\theta)$, and $v_y = v_{per}\sin(\theta)$. The weight of each trajectory is proportional to $w(t_0, v_{per}) = w(0)\overline{w}(1)$ [47]. Here $w(0)$ is the tunneling rate in the quasistatic approximation and $\overline{w}(1) = (2|I_{p1}|)^{1/2}/(\epsilon\pi)\exp[-v_{per}^2(2|I_{p1}|)^{1/2}/\epsilon]$ is the quantum-mechanical transverse velocity distribution.

The initial condition of the second, i.e., the bound electron is determined by assuming that the electron is in the ground state of He^+ and that its initial distribution is a microcanonical distribution [37,48].

NUMERICAL RESULTS AND DISCUSSIONS

Under the condition of the experiment [24], the recoil momentum of the ion, $\mathbf{P}$, satisfies $\mathbf{P} \approx -\mathbf{p}_e$ or $-(\mathbf{p}_{e1} + \mathbf{p}_{e2})$ corresponding to singly or doubly ionized ions, respectively. Here $\mathbf{p}_e$ is the momentum of the ionized electron for single ionization, and $\mathbf{p}_{e1}$ and $\mathbf{p}_{e2}$ are the momenta of the two ionized electrons for double ionization, respectively. We need to calculate the momentum distribution of the ionized electrons. The parameters for our calculation are chosen as $I_{p1} = 0.9$ a.u. (24.12 eV), $I_{p2} = 2$ a.u. (54.4 eV), $\omega = 0.05642$ a.u. ($\lambda_1 = 800$ nm) and $F = 0.0935$ a.u., 0.141 a.u., and 0.174 a.u., corresponding to $I = 2.9 \times 10^{14}$ W/cm^2, 6.6×10^{14} W/cm^2, and 1.0×10^{15} W/cm^2, respectively. The calculation of the single ionization is quite trivial. But the calculation of the double ionization is a little complicated. In the first step of our computation, $(1-2) \times 10^5$ points are randomly distributed in the parameter volume $-\pi/2 < \phi_0 < \pi/2$, $v_{per} > 0$, and $0 < \theta < 2\pi$, where $\phi_0 = \omega t_0$. The trajectories are traced until at least one electron has moved to such a position that $r_i > 200$. About 300 trajectories are found to lead to double ionization in our calculations. In the second step, the parameter volume is carefully chosen according to the parameters obtained in the double-ionization cases [37]. It is pointed out in Ref. [37] that most double-ionization yields come from the region $-0.2 < \phi_0 < 0.4$ with a tail up to $\phi_0 = 1.2$. Moreover, the parameter volume of the initial perpendicular velocity component also gets reduced depending on the calculations of the first step. Finally, about $(1-2) \times 10^4$ double-ionization cases are obtained in about $(1-2) \times 10^6$ random traces. Then these cases are traced until $t_f = 13T$ to obtain the distribution of the momenta of the electrons; here T is the period of the laser field. In the calculations, the field strength is a constant during $t_0 < t < 10T$ and is turned off in a cosine-squared shape during the last three periods.

Figure 1 shows the momentum distributions of singly ionized He parallel and perpendicular to the laser polarization. It is interesting to note that the distributions of the momenta parallel to the polarization display a double-hump structure, similar to that for double ionization. For comparison, the momentum distribution obtained without considering the interaction between the tunneled electron and the core is also shown in Fig. 1, which presents a single-peak structure, in contrast. This comparison clearly shows that the double-hump structure in the distribution of single ionization also appears because of the interaction between the electron and the core, i.e., the recollision. This can be seen more clearly in Fig. 2 which shows the distribution of phase ϕ_0 corresponding to different final momenta. Since the momentum values obtained in our simulation are continuous, the momentum labeled in Fig. 2, for example, $p_e = 0.35$ a.u., means the momentum in the interval $[p_e - \delta p, p_e + \delta p]$, where δp is chosen as 0.1 a.u. As stated above, we choose $-\pi/2 < \phi_0 < \pi/2$ in the simulation and obtain the distribution. However, the momentum distributions shown in Fig. 1 and Fig. 3 are obtained by reflecting the distribution relative to 0 and adding them together. It is well known that, in the semiclassical picture, the tunneled electron, with momentum equal to zero, is ionized around the peak of the laser field, i.e., $\phi_0 = 0$, and has the largest probability, which gives the single peak located at zero in the distribution. But with the rescattering effect included, most of the electrons ionized near the peak of the field will return to the core with nonzero momentum, interact with the core (rescattering) and the field and finally acquire nonzero momenta. It can thus be seen in Fig. 2 that, when the momentum changes from zero to 0.25 a.u., the peak of the distribution shifts from about -0.1 to about zero and the probability (the area under the curve) also increases. When the momentum increases to 0.35 a.u., the location of the peak moves to about 0.05 and the probability reaches the maximum, corresponding to the location of the peak at $p_e = 0.35$ a.u. in Fig. 1(c). If the momentum increases further, the peak of the distribution shifts further but the probability begins to decrease.

Our results are qualitatively consistent with the experimental data [24,25]. The experimental results, however, did not indicate the double-hump structure in the momentum distribution along the laser polarization, possibly due to limited resolution. There are several reasons for the discrepancy between our simulation and the experiments. First, a constant

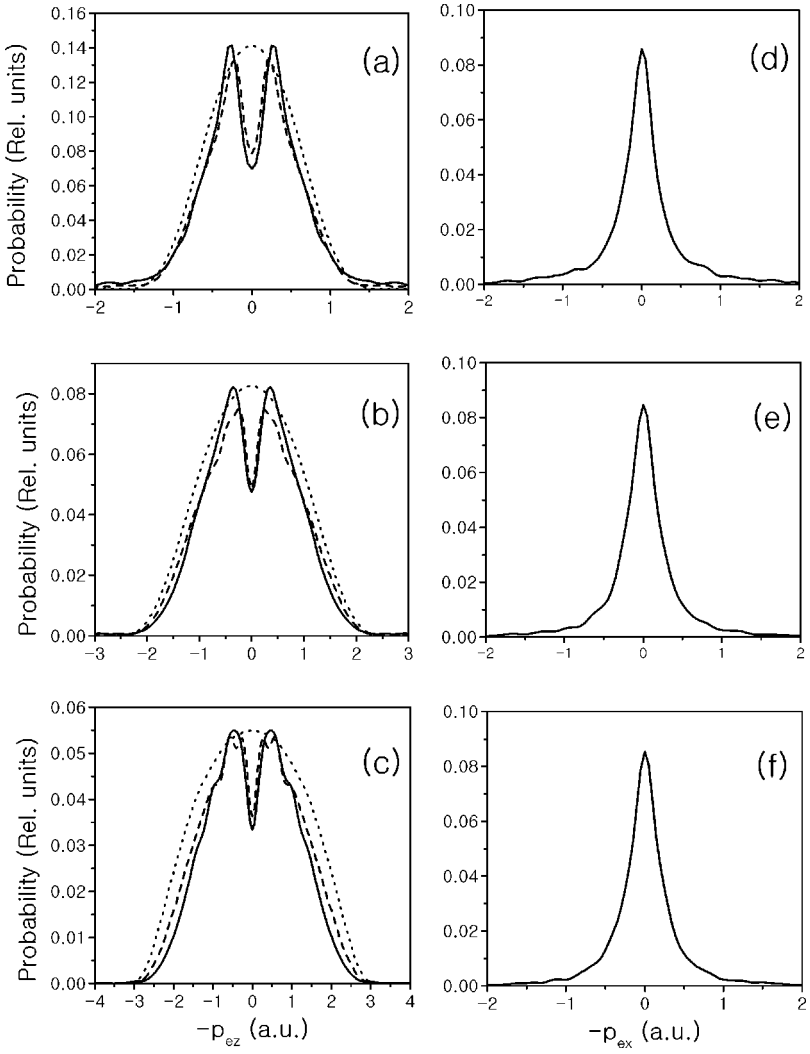

FIG. 1. From top to bottom, momentum distribution of He^+ ions in the parallel direction [(a),(c),(e)] and perpendicular direction [(b),(d),(f)] to the laser polarization. (a),(b) $I = 2.9\times10^{14}$ W/cm^2; (c),(d) 6.6×10^{14} W/cm^2 and (e),(f) 1.0×10^{15} W/cm^2. Solid line, considering rescattering; dotted line, without rescattering; dashed line, calculation with Coulomb approximation instead of the bound electron (see text).

amplitude field is used in our simulation. In fact, the contributions at different times during the laser pulse and at different positions in the focusing volume with different laser intensities may smear out the theoretical predicted structures in actual experiments. Second, the resolution of the measurement in the experiment was probably not high enough. Since the space between the two peaks in the distribution is small, as seen in Fig. 1, it may be difficult to resolve the detailed structure in experiments. Third, the semiclassical model is believed to overestimate the rescattering effect since the interaction between the electron and the field is treated classically without considering the quantum effects such as diffusion [8]. Fourth, compared to a high-energy electron with large momentum, a low-energy electron with small momentum has a higher probability to undergo inelastic collisions with the ion. It may then recombine with the ion or excite the bound electron and be simultaneously captured to form a doubly excited bound state of He that is only classically allowed. This can be confirmed by examining the phase distribution that leads to atomic He after evolution as shown in Fig. 2 (thick solid line). It is clearly seen that the phases leading to recombination focus in the region where the momentum is small. This classical recombination effect indeed deepens the valley between the maxima in the momentum distribution. However, it will not completely smear out the characteristics of the distribution if the classical recombination effect is avoided because of the fact that the main contribution to the peak of the momentum distribution is from the cases with phases around zero. This has the highest probability and is slightly influenced by the classical recombination effect (in the quantum picture, the electron also has some probability to recombine with the ion). Furthermore, to avoid the formation of the doubly excited bound state of He, further calculations have been done by using the Coulomb approximation to simulate the potential of He^+ instead of the bound electron. These results are also presented in Fig. 1 and show slightly shallower valleys and closer distances between the peaks in the momentum distributions. It is noted that a similar calculation of the momentum distribution for single ionization of Ne is reported in Ref. [49], where no double-hump structure in the momentum distribution was observed. However, because they use a classical Monte Carlo method to calculate the ionization process, the tunneling ionization that plays a very important role cannot be included and the distribution, especially in the small momentum part, is not correct for comparison with experimental result [49]. In addition, it is clearly seen in Fig. 1 that the width of the distribution obtained by including rescattering is narrower than

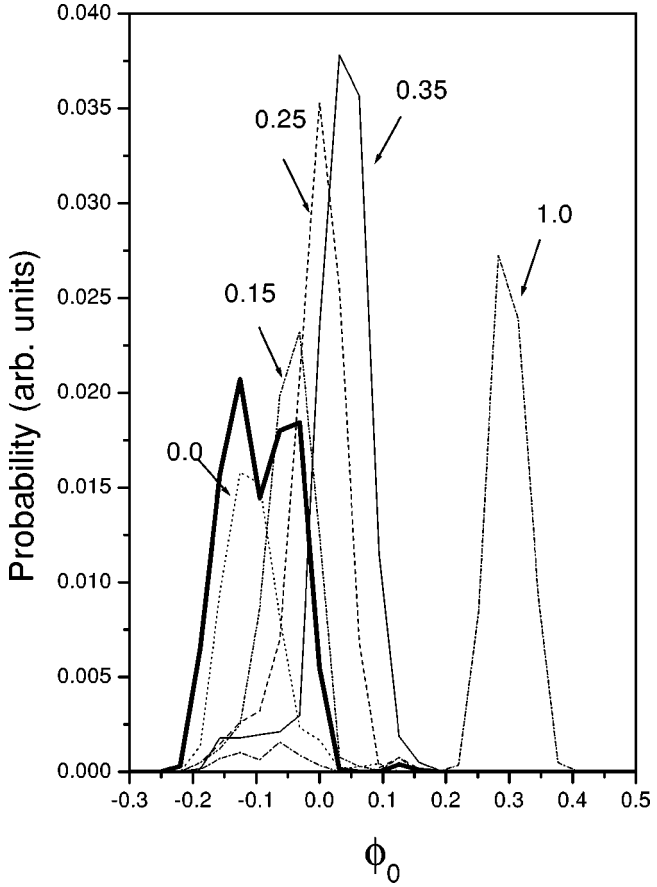

FIG. 2. Distribution of phase ϕ_0 corresponding to different momenta except the thick solid line which is for the recombination (see text). The numbers shown represent the electron momentum (in atomic units).

that of the distribution without considering rescattering and is more consistent with the experimental data [24,25]. In our opinion, this is also the consequence of the interaction between the electron and the ionic potential. Since the ionic potential is an attractive one, it will reduce the momentum of the ejected electron and then leads to a narrower momentum distribution. On the other hand, the excitation of the bound electron by the inelastic collision with the tunneled electron and the recombination of the tunneled electron will also reduce the width of the momentum distribution. In summary, the double-hump effect of single ionization may be overestimated in the semiclassical model due to its classical aspect. However, it can still be seen in Fig. 1 of Ref. [24] that there is at least a plateau structure around the center. This kind of effect needs to be examined in future experiments.

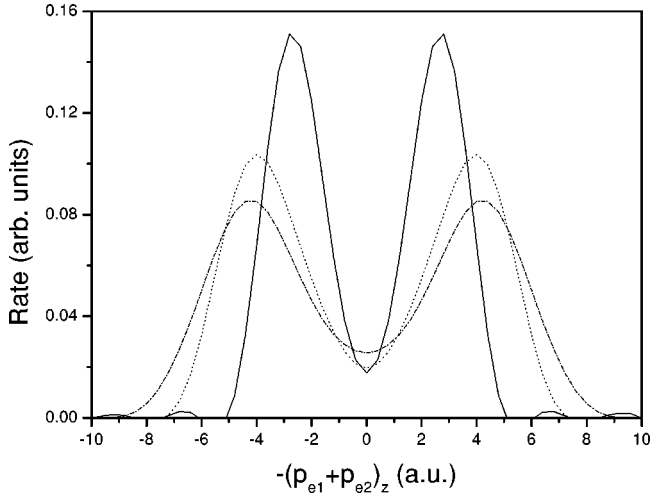

FIG. 3. He^{2+} recoil-ion momentum distributions. Solid line, 2.9×10^{14} W/cm^2; dotted line, 6.6×10^{14} W/cm^2; and dash-dotted line, 1.0×10^{15} W/cm^2.

We next turn our discussion to the double-ionization process. Figure 3 shows the distributions of momenta for double ionization. The results are qualitatively consistent with the experimental data presented by Weber *et al*. [24], whereas in the experiment the double-peak structure is much less pronounced. All the distributions of momenta parallel to the polarization display the structure of well separated double peaks, which is believed to be a consequence of the rescattering mechanism of the nonsequential double ionization. It can be understood as follows. For simplification, it is assumed that only the electron that tunnels out at t_a has enough kinetic energy to ionize the bound electron when it returns back to the ion at time t_b (only consider $-T/4<t_a<T/4$ according to the symmetry of the laser field as stated above). It is known that in the absence of an external field, the sum of the momentum of the two electrons after impact ionization is a single-hump distribution with a central maximum [50]. In the presence of the external field the ionized electrons will be accelerated by the field. Then the maximum of the sum-momentum distribution moves up or downwards (according to $-T/4<t_a<T/4$ or $T/4<t_a<3T/4$) by a magnitude dependent on the time at which the electrons are ionized and thus finally forms a double-hump structure with a central minimum. Moreover, it can be seen from Fig. 3 that when the intensity increases, the absolute value of the momentum with maximum probability increases. This is reasonable since more intense field will accelerate the electron with larger momentum.

Another interesting feature that can be observed from Fig. 3 is that when the intensity decreases, the minimum between the two peaks also decreases relatively. This can be understood by examining Fig. 4 that shows the angular distributions of the two emitted photoelectrons in double ionization. Here the asymmetry with respect to 90° (perpendicular to the polarization direction of the field) in the figures is due to our choice of the phase in the interval $\phi_0\in[-\pi/2,\pi/2]$. The angular distribution of the electron with initial phase in $[\pi/2,3\pi/2]$ will be the mirror image of that with respect to 90°. So the total angular distribution, i.e., the distribution observed in the experiment, is the sum of the two contributions and will be symmetrical with respect to 90°. The distribution with $I=2.9\times10^{14}$ W/cm^2 is more concentrated on the negative direction than those with $I=6.6\times10^{14}$ W/cm^2 and 1.0×10^{15} W/cm^2. This effect can be understood as follows: neglecting the core potential, the final momentum of the ionized electron can be expressed as

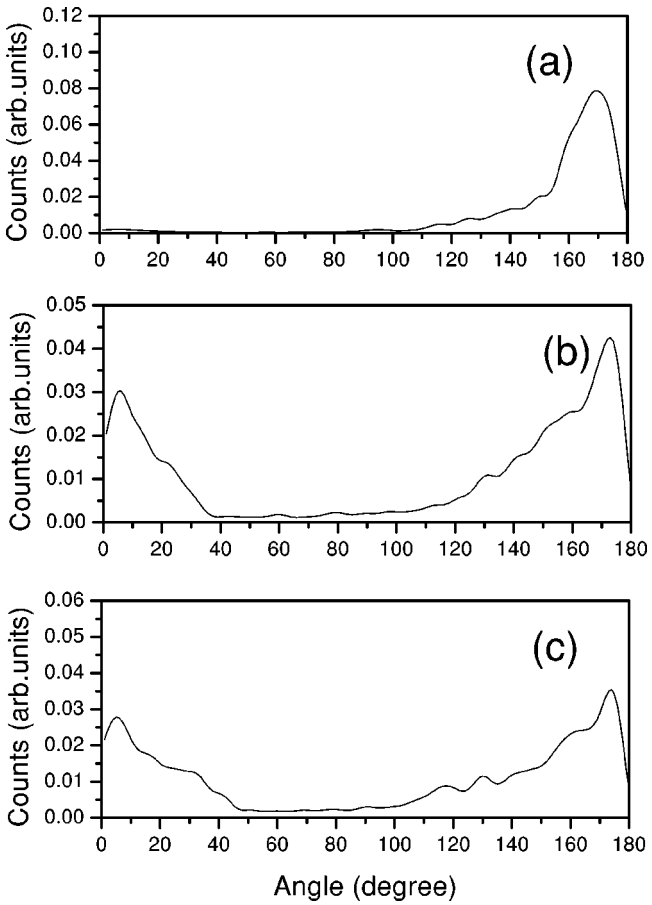

FIG. 4. The angular distributions of the two emitted photoelectrons in double ionization at laser intensities (a) 2.9×10^{14} W/cm^2, (b) 6.6×10^{14} W/cm^2 and (c) 1.0×10^{15} W/cm^2.

$$\mathbf{p}=-\frac{q}{\omega}\mathbf{F}\sin\omega t_c+\mathbf{p}_c, \tag{2}$$

where t_c is the collision time and $\mathbf{p}_c$ is the momentum of the electron just after the collision. For simplification, we assume

$$p_c=\sqrt{2(3.17U_p-I_{p2})}, \tag{3}$$

which means that all the excess energy is gained by only one electron. In the case of $I=2.9\times10^{14}$ W/cm^2, we have $F/\omega=1.66$ a.u. and $p_c=0.59$ a.u. Since the phase ωt_c is mainly in the interval from $3\pi/2$ to 2π, i.e., $\sin\omega t_c<0$, the final momenta of electrons are mainly in the negative direction. This gives rise to the shift of the maximum to the opposite direction in the angular distribution of He^{2+} compared with that of single ionization [45]. In fact, the excess energy is shared by two electrons, and consequently almost all the electrons will be driven to the negative direction in this condition. In the cases of $I=6.6\times10^{14}$ W/cm^2 and 1.0×10^{15} W/cm^2, we have $F/\omega=2.5$ a.u.,3.07 a.u. and $p_c=2.43$ a.u., 3.31 a.u. Thus more and more of the ionized electrons cannot be driven to the negative direction as the intensity increases. This leads to the fact that the minimums between the peaks become less pronounced with increasing intensity.

However, it is obvious that this trend is not consistent with the experimental observations [24]. In the experiments, on the contrary, the minimum between the peaks increases relatively as the intensity decreases. This discrepancy indicates that when the intensity decreases to a value well below the saturation intensity, the simple rescattering ionization mechanism does not dominate the process. Other mechanisms giving rise to central peak distribution of the momentum parallel to the polarization should be introduced. For example, the process of rescattering excitation with subsequent tunneling has been shown to become important for an Ar target as the intensity decreases [28].

Similar to the situation in single ionization, it may happen that the cross section of the recapture of one electron by the ion is overestimated in the classical calculations and this effect will deepen the valley as the intensity decreases which puts our conclusions on a weak ground. We examine the probability of recapture by counting the number of events for which the total energies of both electrons have been once above zero during the evolution but finally end up as single ionization. This number is quite small and increases as the intensity decreases, but is in any case less than 10% of all double-ionization events when the intensity is 2.9×10^{14} W/cm^2. Thus, this limitation of the model should not influence the conclusion obtained above.

The momentum correlation between the two emitted electrons is also shown in Fig. 5 that presents the density plot of the distribution of the momentum components parallel to the polarization of the laser field. It is clearly seen that the emitted electrons have a strong tendency to fly to the same side of the ion in the polarization direction, which is consistent with the experiments [27] and previous simulations [41,46]. In addition, when the intensity decreases, the emitted electrons show an even stronger trend to acquire similar momenta parallel to the laser field. This is also consistent with the above analysis.

Figure 6 presents the momentum correlation between the electrons with different relative transverse momenta. Here the relative transverse momentum is defined as $\Delta p=[(p_{1x}-p_{2x})^2+(p_{1y}-p_{2y})^2]^{1/2}$. A dependence of the correlation pattern on the transverse momentum can be observed. Comparing Fig. 6 with Fig. 5(b), if the relative transverse momentum is large, the density along the diagonal line increases, which means that both the electrons are more likely to have similar parallel momenta. In contrast, if the relative transverse momentum is small, the density along the diagonal line decreases, indicating that the electrons tend to have different parallel momenta. This dependence can be explained as the repulsion effect in the correlation between the emitted electrons [29,51].

CONCLUSIONS

In summary, by using a semiclassical rescattering model, we have calculated the momentum distribution of recoil ions from laser induced single and double ionization. It has been

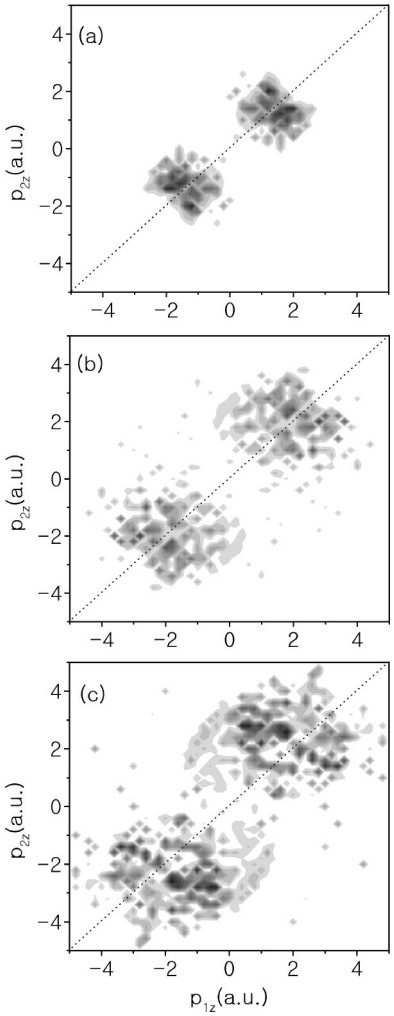

FIG. 5. Density plot of the distribution of the momentum components of electron one and two parallel to the laser polarization direction.

found that in both cases of single and double ionization, the distributions of the momentum parallel to the polarization show a double-hump structure. Analysis shows that the double-hump structure in single ionization is also the consequence of the rescattering, i.e., the interaction between the tunneled electron and the potential of the core, similar to that in the case of double ionization. The result is compared with experiments and the limitations of the model are discussed. For double ionization, the calculations show that the minimum in the center of the distribution of the momentum parallel to the laser polarization decreases as the laser intensity decreases. This is not consistent with the experimental observations indicating a contrary tendency. Thus, it can be concluded that, when the intensity of the laser decreases, the contribution from the rescattering ionization process of the second electron will diminish and other processes, which are not included in the present model, may begin to dominate. In addition, the correlated emission of electrons in double ionization is observed in the density plot of the distribution of the momentum components, of both the emitted electrons, parallel to the polarization. Comparison with experiments yields qualitative consistency. Finally, the evidence of the repulsion between the emitted electrons is observed in the momentum correlation between the electrons with different relative transverse momenta.

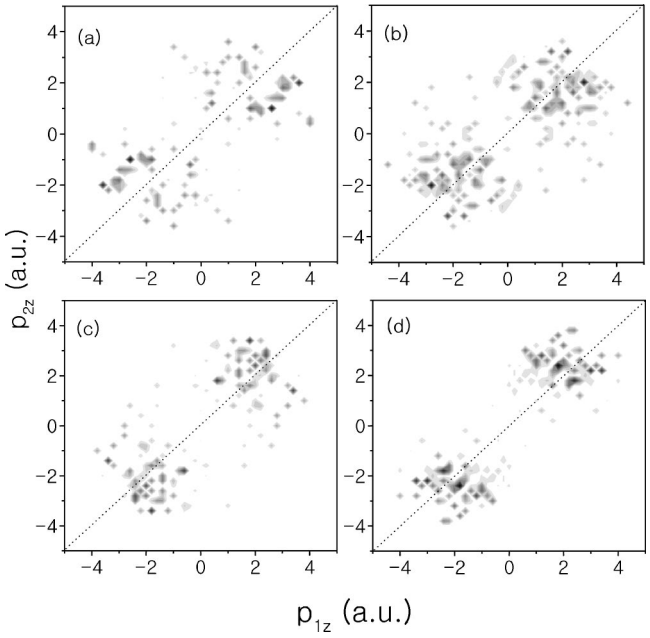

FIG. 6. Momentum correlation between the emitted electrons with different relative transverse momentum Δp. (a) $\Delta p < 0.5$ a.u.; (b) $0.5 < \Delta p < 1.0$ a.u.; (c) $1.0 < \Delta p < 1.5$ a.u., (d) $\Delta p > 1.5$ a.u.

ACKNOWLEDGMENTS

The authors would like to thank Dr. Jung Hoon Kim for helpful discussions and Dr. Umesh for careful reading of our paper and many suggestions. This work was supported by the Ministry of Science and Technology of Korea through the Creative Research Initiative Program and partially supported by Important Fundamental Research Project in China.

[1] J.L. Krause, K.J. Schafer, and K.C. Kulander, Phys. Rev. Lett. **68**, 3535 (1992).
[2] P.B. Corkum, Phys. Rev. Lett. **71**, 1994 (1993).
[3] G.G. Paulus, W. Nicklich, F. Zacher, P. Lambropoulos, and H. Walther, J. Phys. B **52**, L249 (1996).
[4] W. Becker, A. Lohr, and M. Kleber, J. Phys. B **27**, L325 (1994).
[5] M. Lewenstein, K.C. Kulander, K.J. Schafer, and P.H. Bucksbaum, Phys. Rev. A **51**, 1495 (1995).
[6] D. Bao, S.G. Chen, and J. Liu, Appl. Phys. B: Lasers Opt. **62**, 313 (1996).
[7] B. Hu, J. Liu, and S.G. Chen, Phys. Lett. A **236**, 533 (1997).

[8] J. Chen, J. Liu, and S.G. Chen, Phys. Rev. A **61**, 033402 (2000).
[9] A. L'Huiller *et al.*, Phys. Rev. A **27**, 2503 (1983).
[10] D.N. Fittinghoff *et al.*, Phys. Rev. Lett. **69**, 2642 (1992).
[11] B. Walker *et al.*, Phys. Rev. Lett. **73**, 1227 (1994).
[12] T. Brabec, M.Y. Ivanov, and P.B. Corkum, Phys. Rev. A **54**, R2551 (1996).
[13] J.B. Watson *et al.*, Phys. Rev. Lett. **78**, 1884 (1997).
[14] A. Becker and F.H.M. Faisal, J. Phys. B **29**, L197 (1996).
[15] A. Becker and F.H.M. Faisal, J. Phys. B **32**, L335 (1996).
[16] K.J. LaGattuta and J.S. Cohen, J. Phys. B **31**, 5281 (1998).
[17] K.C. Kulander, J. Cooper, and K.J. Schafer, Phys. Rev. A **51**, 561 (1995).
[18] D.N. Fittinghoff *et al.*, Phys. Rev. A **49**, 2174 (1994).
[19] M.Yu. Kuchiev, J. Phys. B **28**, 5093 (1995).
[20] B. Sheehy *et al.*, Phys. Rev. A **58**, 3942 (1998).
[21] W.C. Liu *et al.*, Phys. Rev. Lett. **77**, 520 (1999).
[22] V. Schmidt, *Electron Spectrometry of Atoms using Synchrotron Radiation* (Cambridge University Press, Cambridge, England, 1997).
[23] A. Becker and F.H.M. Faisal, Phys. Rev. A **59**, R1742 (1999).
[24] Th. Weber *et al.*, Phys. Rev. Lett. **84**, 443 (2000).
[25] R. Moshammer *et al.*, Phys. Rev. Lett. **84**, 447 (2000).
[26] Th. Weber *et al.*, J. Phys. B **33**, L127 (2000).
[27] Th. Weber *et al.*, Nature (London) **405**, 658 (2000).
[28] B. Feuerstein *et al.*, Phys. Rev. Lett. **87**, 043003 (2001).
[29] R. Moshammer *et al.*, Phys. Rev. A **65**, 035401 (2001).
[30] A. Becker and F.H.M. Faisal, Phys. Rev. Lett. **84**, 3546 (2000).
[31] U. Eichmann *et al.*, Phys. Rev. Lett. **84**, 3550 (2000).
[32] B. Witzel, N.A. Papadogiannis, and D. Charalambidis, Phys. Rev. Lett. **85**, 2268 (2000).
[33] B. Feuerstein *et al.*, J. Phys. B **33**, L823 (2000).
[34] M. Lein *et al.*, Phys. Rev. Lett. **85**, 4707 (2000).
[35] H.W. van der Hart and K. Burnett, Phys. Rev. A **62**, 013407 (2000).
[36] J. Chen *et al.*, Phys. Rev. A **63**, 011404(R) (2001).
[37] L.B. Fu *et al.*, Phys. Rev. A **63**, 043416 (2001).
[38] V.R. Bhardwaj *et al.*, Phys. Rev. Lett. **86**, 3522 (2001).
[39] G.L. Yudin and M.Yu. Ivanov, Phys. Rev. A **63**, 033404 (2001).
[40] K. Sacha and B. Eckhardt, Phys. Rev. A **64**, 053401 (2001).
[41] S.P. Goreslavskii *et al.*, Phys. Rev. A **64**, 053402 (2001).
[42] E.R. Peterson and P.H. Bucksbaum, Phys. Rev. A **64**, 053405 (2001).
[43] M. Dammasch *et al.*, Phys. Rev. A **64**, 061402(R) (2001).
[44] R. Lafon *et al.*, Phys. Rev. Lett. **86**, 2762 (2001).
[45] J. Chen *et al.* Phys. Rev. A **66**, 043410 (2002).
[46] L.B. Fu *et al.*, Phys. Rev. A **65**, 021406(R) (2002).
[47] N.B. Delone and V.P. Krainov, J. Opt. Soc. Am. B **8**, 1207 (1991).
[48] J.S. Cohen, Phys. Rev. A **26**, 3008 (1982).
[49] C.R. Feeler and R.E. Olson, J. Phys. B **33**, 1997 (2000).
[50] A.P.R. Ran, Phys. Rep. **110**, 369 (1984).
[51] M. Weckenbrock *et al.*, J. Phys. B **34**, L449 (2001).